

A Spatiotemporal Profile of In Vivo Cerebral Blood Flow Changes Following Intranasal Oxytocin in Humans

Yannis Paloyelis, Orla M. Doyle, Fernando O. Zelaya, Stefanos Maltezos, Steven C. Williams, Aikaterini Fotopoulou, and Matthew A. Howard

ABSTRACT

BACKGROUND: Animal and human studies highlight the role of oxytocin in social cognition and behavior and the potential of intranasal oxytocin (IN-OT) to treat social impairment in individuals with neuropsychiatric disorders such as autism. However, extensive efforts to evaluate the central actions and therapeutic efficacy of IN-OT may be marred by the absence of data regarding its temporal dynamics and sites of action in the living human brain.

METHODS: In a placebo-controlled study, we used arterial spin labeling to measure IN-OT-induced changes in resting regional cerebral blood flow (rCBF) in 32 healthy men. Volunteers were blinded regarding the nature of the compound they received. The rCBF data were acquired 15 min before and up to 78 min after onset of treatment onset (40 IU of IN-OT or placebo). The data were analyzed using mass univariate and multivariate pattern recognition techniques.

RESULTS: We obtained robust evidence delineating an oxytocinergic network comprising regions expected to express oxytocin receptors, based on histologic evidence, and including core regions of the brain circuitry underpinning social cognition and emotion processing. Pattern recognition on rCBF maps indicated that IN-OT-induced changes were sustained over the entire posttreatment observation interval (25–78 min) and consistent with a pharmacodynamic profile showing a peak response at 39–51 min.

CONCLUSIONS: Our study provides the first visualization and quantification of IN-OT-induced changes in rCBF in the living human brain unaffected by cognitive, affective, or social manipulations. Our findings can inform theoretical and mechanistic models regarding IN-OT effects on typical and atypical social behavior and guide future experiments (e.g., regarding the timing of experimental manipulations).

Keywords: Arterial spin labeling, Cerebral blood flow, Intranasal, Oxytocin, Pharmacodynamics, Resting state

<http://dx.doi.org/10.1016/j.biopsych.2014.10.005>

Animal research has demonstrated that oxytocin (OT) plays a key role in the development and regulation of mammalian social behavior (1–7). In the absence of suitable radioligands, designs using intranasal sprays to manipulate OT levels in the brain (8) or to investigate the effects of polymorphisms in the OT receptor gene (9) have confirmed a similar role in humans (10–17). An increasing number of clinical trials have explored the therapeutic value of intranasal oxytocin (IN-OT) for neuropsychiatric disorders characterized by social impairment, such as autism, schizophrenia, and anorexia, with promising initial results (10,18–26). However, this effort is marred by the absence of data relating to the pharmacodynamics of IN-OT in the human brain.

As a consequence, studies still determine experimental parameters based on assumptions derived from the temporal profile of changes in the concentration of vasopressin in the cerebrospinal fluid (CSF) after intranasal administration (27). However, translating this work to studies using IN-OT faces two obstacles. First, despite their structural similarity, vasopressin and OT are different neuropeptides with distinct

neurophysiology (8,28,29). Second, although the more recent demonstration that IN-OT also increases CSF OT concentration in adult male volunteers (30) is promising, there is dissociation between the concentration of a neuropeptide in the CSF and its availability in brain tissue (31). We need to understand the temporal changes in brain physiology caused by IN-OT to optimize future studies.

Equally, we need to understand the spatial distribution of IN-OT effects in humans. There are three main reasons this understanding is currently hindered. First, the distribution and concentration of OT receptors underpin interspecies and intraspecies differences in social behavior (32), precluding direct translation of information across species. To date, the sole evidence regarding the distribution of OT receptors in human brain comes from the study of a small number of postmortem brains of mainly elderly donors (33–35). Although valuable, these studies provide only a static snapshot of a dynamic system using radioligands for which the receptor specificity is not fully determined (35,36). Second, task-based blood oxygen level-dependent (BOLD) functional magnetic

SEE COMMENTARY ON PAGE 631

resonance imaging (fMRI) studies cannot address this question because they identify relative changes between experimental and control conditions and are not sensitive to a single physiologic parameter (37,38). Consequently, any observed effects are uniquely confined to the neural network engaged in a given task. Third, animal studies demonstrate that different social stimuli may elicit different release profiles of endogenous OT (28). Conclusions regarding changes in brain function induced by IN-OT are limited to the stimulus class employed. More recent “resting-state” BOLD fMRI studies have circumvented some of these issues by focusing on changes in functional connectivity following IN-OT (39,40). Resting-state fMRI provides a promising alternative but cannot quantify changes in brain physiology directly.

We sought to understand the spatial and temporal profile of neurophysiologic changes in the 25–78 minutes following the onset of IN-OT administration (compared with placebo) in the human brain. We used arterial spin labeling (41,42) to measure *in vivo* changes in brain physiology unaffected by concomitant cognitive, affective, or social manipulations. Arterial spin labeling is a noninvasive pharmacodynamic biomarker (43–48) that provides quantitative measures of the effects of acute doses of psychoactive drugs on regional cerebral blood flow (rCBF), with high spatial resolution and excellent temporal reproducibility (37,43,49). Changes in rCBF are likely to reflect changes in neuronal activity, rather than simple vascular effects (50–55).

We expected to observe increases in rCBF over mainly limbic areas previously identified to express OT receptors in human postmortem brains (33–35) and brain areas involved in social-emotional processing that are functionally linked with regions expressing OT receptors, such as the insula and inferior frontal gyrus (56–58). At least 100-fold higher affinity is shown by OT for OT receptors compared with vasopressin receptors (29,36,59). We mapped the distribution of effects of IN-OT using conventional mass univariate voxel-by-voxel analysis, allowing inferences regarding local regions. In the absence of an *a priori* pharmacodynamic model, we used multivariate pattern recognition (PR) on rCBF maps (60) to elucidate temporal dynamics. When the pharmacologic intervention elicits correlated, spatially distributed effects (37,44,45,61) as IN-OT does (28,62), PR offers increased sensitivity compared with conventional mass univariate approaches. The overall pattern of rCBF changes at each temporal interval can be reduced by PR into a single metric—the probability that an rCBF image belongs to a particular class (here, IN-OT or placebo). Using these predictive probabilities, we created pharmacodynamic profiles of changes in brain physiology following IN-OT or placebo.

METHODS AND MATERIALS

Participants

We recruited 32 healthy men (IN-OT group, $n = 16$, mean age (SD) = 24.23 (1.75) years; placebo group, $n = 16$, mean age = 25.78 (4.44) years; $t_{30} = 1.30$, $p = .21$) based on previous power analyses (63). Participants were screened for psychiatric conditions using Symptom Checklist-90-Revised (64) and Beck Depression Inventory-II (65) questionnaires, did not take

any prescribed drugs, tested negative on a urine screening test for drugs of abuse, and consumed <28 units of alcohol per week and <5 cigarettes per day. Both parents of participants were white European to reduce genetic background variability. Participants abstained from alcohol and heavy exercise for 24 hours and abstained from any beverage or food in the 2 hours before scanning in the morning. Participants gave written informed consent. King’s College London Research Ethics Committee (PNM/10/11-160) approved the study.

Design, Materials, and Procedure

We employed a single-blinded, placebo-controlled design with two independent study arms. Before taking part, all participants were informed they would receive a neuropeptide and remain blinded to its name and that they might receive placebo until the postsession debriefing; 50% received IN-OT, and 50% received placebo. We obtained two baseline cerebral blood flow (CBF) images before participants came out of the scanner to receive 40 IU of IN-OT (Syntocinon; Novartis, Basel, Switzerland) or placebo (same composition as Syntocinon except for OT). We used 40 IU, the highest clinically applicable safe dose administered to human volunteers [e.g., in 14% of studies until 2011 (66) and still being used (15)] to maximize power. Use of this dose also ensured comparability with the study of Born *et al.* (27) on vasopressin in the CSF using 40 IU as the minimum dose.

Participants self-administered one puff (4 IU) of IN-OT (or placebo) every 30 seconds, alternating between nostrils. The administration phase lasted approximately 9 minutes including a 3-minute rest at the end. Participants returned to the scanner for two anatomic scans followed by eight CBF images spanning 25–78 minutes from the onset (henceforth called postadministration scans) of nasal spray administration (Figure 1A). Participants were instructed to lie still and maintain their gaze on a centrally placed fixation cross during scanning. We assessed participants’ levels of alertness (anchors: alert-drowsy) and excitement (anchors: excited-calm) using visual analog scales before acquiring each CBF image. The subjective ratings of one participant from the IN-OT group were lost because of a technical issue.

Image Acquisition and Preprocessing

Images were acquired using a Signa HDx 3.0T magnetic resonance imaging scanner (General Electric, Milwaukee, Wisconsin). We employed the pulsed-continuous arterial spin labeling methodology (67). The CBF maps (in standard physiologic units—mL blood/100 g tissue/min) were computed with a spatial resolution of 1 mm × 1 mm × 3 mm. Total acquisition time for each CBF map was 5.5 minutes. We also acquired a T2-weighted fast spin echo high spatial resolution structural image for coregistration and normalization purposes.

We performed the following preprocessing steps (detailed in the Supplement). 1) We removed extracerebral signal from each participant’s T2 volume and created a binary brain mask. 2) We coregistered each CBF image to the corresponding T2 volume for each participant, correcting for interscan movement. 3) We removed extracerebral signal from CBF images by

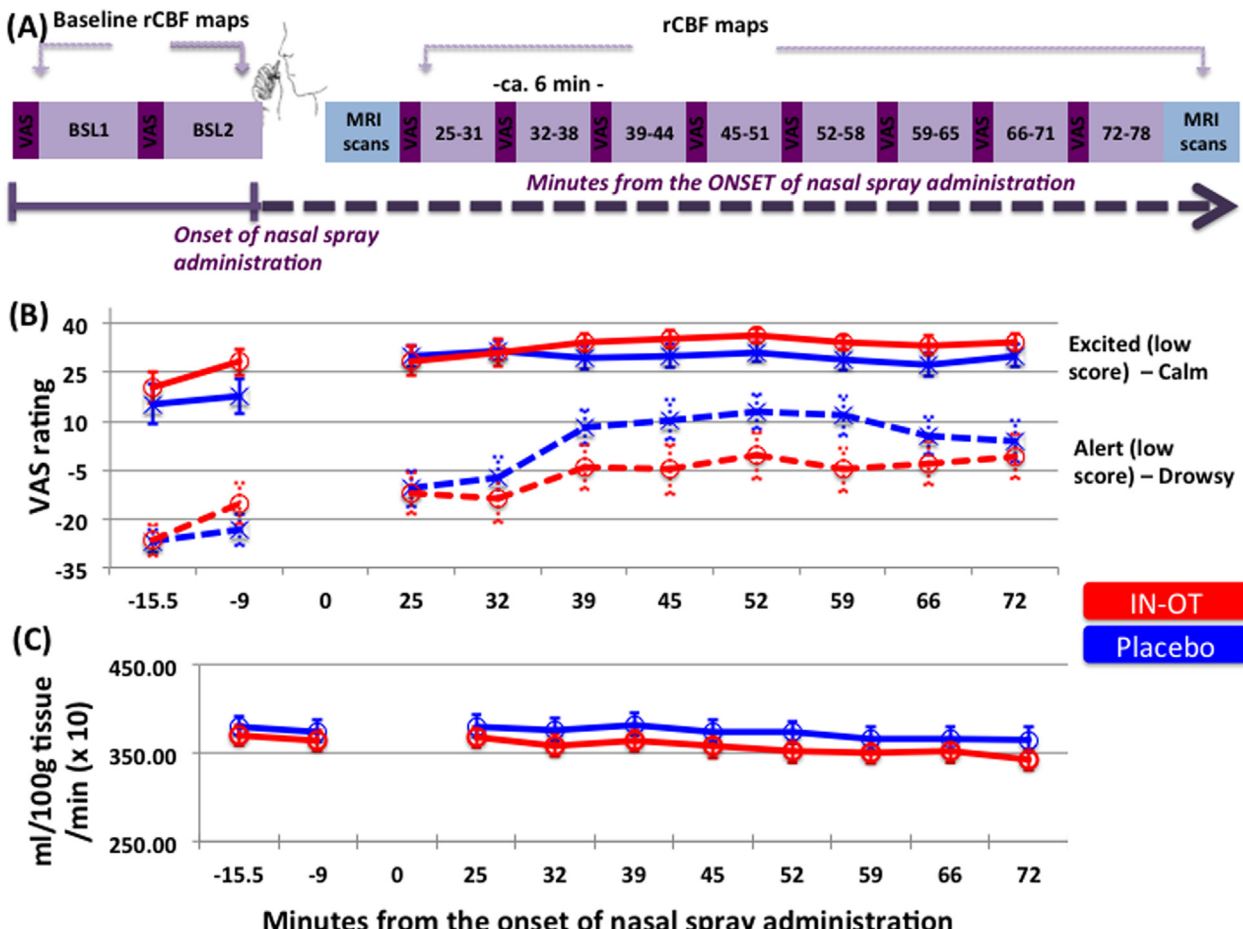


Figure 1. Experimental design, subjective ratings, and global cerebral blood flow values (IN-OT group, $n = 16$; placebo group, $n = 16$). **(A)** Experimental design. **(B)** Overall, participants' levels of alertness (IN-OT, $z = 2.57, p = .010$; placebo, $z = 2.20, p = .028$) and excitement (IN-OT, $z = 2.12, p = .034$; placebo, $z = 1.40, p = .16$) linearly decreased over time. For VAS ratings, we measured the distance of the cursor from one extreme and converted to a score ranging from -50 (alert/excited) to 50 (drowsy/calm), with 0 being the midpoint. **(C)** Global cerebral blood flow values also linearly decreased over time (IN-OT, $z = -2.82, p = .005$; placebo, $z = -2.45, p = .014$). Error bars represent SE. Corrected p values reported. BSL, baseline; IN-OT, intranasal oxytocin; MRI, magnetic resonance imaging; rCBF, regional cerebral blood flow; VAS, visual analog scale.

multiplying them by the binary brain mask. 4) We normalized the T2 volume to the Montreal Neurological Institute 2-mm T2 template, applying the transformation matrix to the coregistered, brain-only CBF images. 5) We smoothed the CBF images using an 8-mm Gaussian kernel. We restricted the search volume to gray matter voxels only using an explicit mask of voxels with a $>.20$ probability of being gray matter.

Global CBF Measures and Subjective Ratings

We extracted global CBF values using MarsBaR (<http://marsbar.sourceforge.net>). We conducted the following analyses (Supplement): First, we performed a nonparametric test for a linear change in global CBF signal and subjective ratings over time (68). Second, we investigated the association between changes in global CBF signal and self-ratings of alertness and excitement over time. Finally, we tested for the effect of treatment on subjective ratings and global CBF signal (averaged over baseline and postadministration scans) with the Treatment (IN-OT, placebo; between-subjects factor) \times

Period (baseline, postadministration; within-subjects factor) term in a mixed 2×2 analysis of variance model implemented in Stata (version 13; StataCorp LP, College Station, Texas), correcting for data dependence (69) and multiple testing using the sequential Holm-Bonferroni correction procedure (70).

Whole-Brain Univariate Analyses: Mapping the Spatial Profile of IN-OT-Induced Changes in rCBF

We implemented an analysis of covariance design to control for baseline differences (71) using a flexible factorial model in SPM8 software (<http://www.fil.ion.ucl.ac.uk/spm/software/spm8/>), specifying the factors Subjects, Treatment, and Period. We used the Treatment \times Period interaction term and an F contrast to test for brain regions where IN-OT led to changes in rCBF regardless of direction in the 25–78 minutes after administration. We conducted cluster-level inferences at $\alpha = .05$, using familywise error (FWE) correction for multiple comparisons from a voxel-level cluster-forming threshold of $Z > 2.3$ (72). The required cluster size threshold for the

F contrast at $\alpha = .05$ was calculated to be $k = 1089$ voxels using Analysis of Functional NeuroImages 3dClustSim (http://afni.nimh.nih.gov/pub/dist/doc/program_help/3dClustSim.html). To understand the nature of the effect, we extracted and plotted the data from each of the identified clusters, adjusting for the Treatment \times Period contrast. To enhance the contrast between rCBF at baseline and after administration, we included global CBF values as nuisance covariates in the general linear model.

PR: Investigating Temporal Dynamics of the Spatial Pattern of IN-OT-Induced Changes in rCBF

We restricted PR analyses to an a priori-defined mask that included brain regions likely to contain oxytocin receptors, based on previous postmortem human brain studies (Supplement). Briefly, PR involves learning a pattern (a “model”) of brain voxels that can distinguish rCBF images as being acquired before or after treatment (our two “classes”). This trained model could be used to assign a label to a new, previously unseen image (“classification”). This procedure is repeated N times, each time using $N-1$ participants to learn the pattern (“training the model”) and applying it to images from the N th (“left-out”) participant (“leave-one-out cross-validation” procedure). We used Gaussian process classification (GPC) (44,61,73) to estimate the probability that a previously unseen image from the N th participant belongs to the posttreatment class (the “predictive probability”) (see the Supplement for more information on the GPC). A predictive probability $>.5$ was used to assign an image to the posttreatment class. The statistical significance of the performance of the model was estimated using permutations (i.e., repeating the above-described procedure after randomly mixing the training image labels 1000 times to test the null hypothesis that the performance is not greater than chance [50%]—of no predictive value).

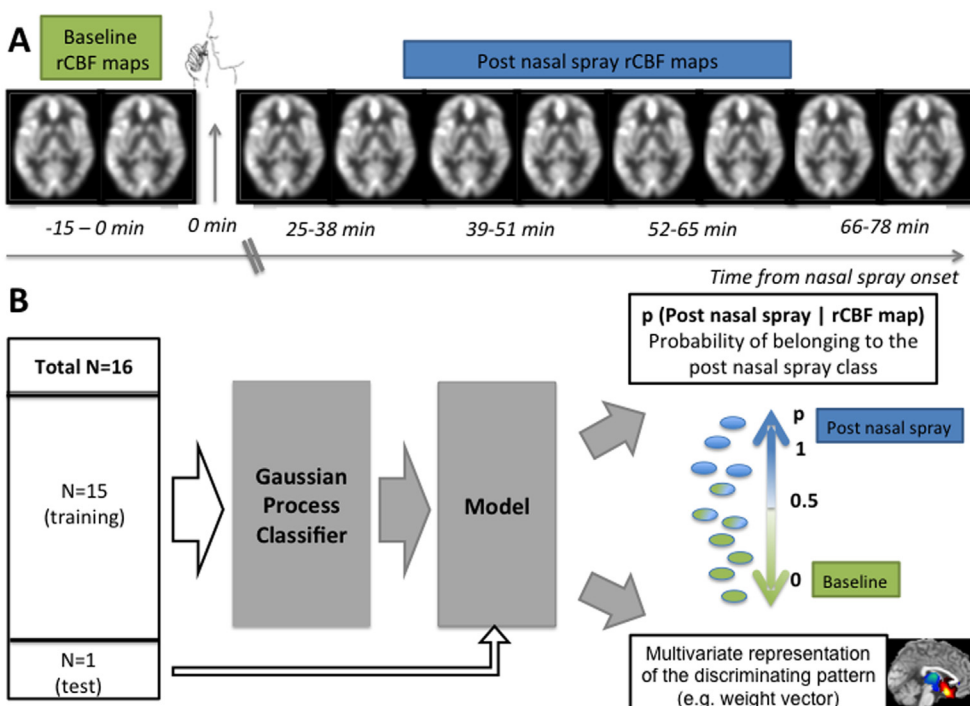


Figure 2 details a schematic representation of GPC analysis. We averaged pairs of consecutive scans to improve the signal-to-noise ratio, potentially improving classification accuracy (45).

We used the predictive probabilities as the main outcome measure and as a proxy to create a pharmacodynamic profile of the IN-OT perfusion effect. We compared scans after administration with baseline for each study arm separately because the administration of IN-OT and placebo to different individuals was expected to inflate the between-group variance, obscuring the sensitivity of GPC to the expected IN-OT effect. Cross-group multivariate classification was not part of our design (see Supplemental Table S1 for results). However, to obtain a formal measure of cross-group classification performance, we implemented a mixed Treatment \times Period (using the seven post-administration subperiods defined by each possible pair of consecutive rCBF images) analysis of variance on predictive probabilities. Finally, we constructed maps to visualize the distributed discriminative spatial pattern of multivariate weights driving the classification.

RESULTS

Global CBF Measures and Subjective Ratings

We observed a general linear decrease over time in participants’ levels of alertness and excitement and in global CBF values in both groups (Figure 1B, C and Supplemental Results). Self-reported levels of alertness and excitement correlated with global CBF values (alertness, $r = .16$, $p = .009$; excitement, $r = .23$, $p < .001$). This association and the significant global decrease in rCBF over time, which might prevent the identification of significant changes in CBF in small regions, provided a suitable rationale for including global CBF

Figure 2. Schematic analysis pipeline. (A) Experimental setup. Indicative rCBF maps are presented for illustration purposes. (B) Training and testing the Gaussian process classifier model on each participant and an illustration of the baseline–post nasal spray continuum. rCBF, regional cerebral blood flow.

as a confounding covariate in the analyses. We did not observe Treatment or Period effects on global CBF values (*Supplemental Results* and *Supplemental Table S2*).

Univariate Analyses: Mapping Spatial Profile of IN-OT-Induced Changes in rCBF

The *F* contrast identified four clusters showing a significant Treatment \times Period interaction in rCBF in the 25–78 minute postadministration interval (*Table 1* and *Figure 3*). Clusters extended over a network of regions including 1) left hemisphere limbic and midbrain/brainstem regions, including amygdala, hippocampus, caudate nucleus, ventral striatum and pallidum, septal and hypothalamic nuclei, substantia nigra, and pontine brainstem nuclei; 2) bilateral dorsal anterior and middle cingulate cortices; 3) inferior frontal gyrus, anterior insula, frontal and parietal opercula, and superior temporal gyrus, extending to the planum temporale and polare and the supramarginal gyrus in inferior parietal cortex; and 4) right hemisphere cerebellum. Directional *T* contrasts for the interaction effect identified the same clusters (clusters 1 and 3, $p_{\text{FWE}} < .001$, $k = 7360$; cluster 2, $p_{\text{FWE}} = .019$, $k = 2114$; cluster 4, $p_{\text{FWE}} = .041$, $k = 1767$). We extracted and plotted data from each of these clusters, observing a crossover interaction pattern where the administration of IN-OT increased rCBF in clusters 1–3 (compared with baseline), whereas the reverse pattern was observed for the placebo group. The opposite pattern was observed in the cerebellum (*Figure 3*).

PR Analyses: Investigating Temporal Dynamics of IN-OT-Induced Changes in rCBF

Classification Accuracies. The classification accuracies for the post IN-OT class (compared with the baseline class) were $>80\%$ at all time intervals and significantly different from chance.

For the post placebo class (compared with baseline), classification accuracies ranged from 38%–81% and did not differ significantly from chance except at the 32–44 minute interval (*Table 2*).

Predictive Probabilities. Statistical analysis of cross-group classification performance using the predictive probabilities confirmed the above-described pattern. We observed a significant main effect for Treatment (but not Period) and a significant Treatment \times Period interaction (*Table 3*, *Figure 4A*). Predictive probabilities were significantly higher for the post IN-OT class compared with post placebo class at 39–51 minute, 45–58 minute, and 52–65 minute intervals. Similarly, there was an effect of Period in the post IN-OT but not the post placebo group. *Figure 4A* shows that the averaged predictive probabilities for the post IN-OT class peaked at the 39–51 minutes post IN-OT interval, followed by a gradual diminution over time. *Figure 4B* shows the multivariate map of the discriminative spatial pattern underpinning classification at the 39–51 minute interval in the post IN-OT and placebo groups.

DISCUSSION

Using arterial spin labeling as a pharmacodynamic biomarker (43–48), we visualized and quantified, for the first time in living human brain, IN-OT-induced changes in rCBF unaffected by concomitant cognitive, affective, or social manipulations. Confirming predictions from postmortem histologic studies (33–35), we delineated an oxytocinergic network comprising regions expected to express OT receptors and that are involved in social cognition and emotion processing (56–58,74–76). Addressing the lack of a temporal dynamics model for the human brain, GPC indicated that IN-OT-induced changes in rCBF were sustained over the posttreatment observation interval of 25–78 minutes

Table 1. Clusters Showing a Significant Treatment \times Period Interaction in rCBF in the 25–78 minute Postadministration Interval (*F* Contrast)

Cluster Description	Hemisphere	<i>k</i>	<i>p</i>	Peak Coordinates			Description
				x	y	z	
Cluster 1							
Caudate nucleus, ventral striatum, pallidum, amygdala, hippocampus, septal nuclei, hypothalamus, ventral midbrain (ventral tegmental area, substantia nigra), pontine tegmentum	Left	1999	<.05	-14	-30	-36	Dorsal midbrain
				-10	-18	-26	Ventral midbrain
				-10	4	2	Pallidum
Cluster 2							
Anterior and middle cingulate cortices	Bilateral	1539	<.05	-2	10	24	Anterior cingulate cortex
				-2	-12	32	Middle cingulate cortex
Cluster 3							
Inferior frontal gyrus, anterior insula, planum polare, transverse temporal gyrus, planum temporale, superior temporal gyrus, inferior parietal cortex-supramarginal gyrus, frontal operculum, parietal operculum	Left	2816	<.05	-50	0	-4	Superior temporal gyrus
				-58	-22	0	Middle temporal gyrus
				-58	-24	6	Superior temporal gyrus
Cluster 4							
Cerebellum	Right	1244	<.05	28	-68	-42	Cerebellum (lobule VIa, crus II)
				14	-66	-42	Cerebellum (lobule VIIIa)
				44	-56	-50	Cerebellum (lobule VIa, crus I)

The required cluster size threshold at $\alpha = .05$ was calculated to be $k = 1089$ voxels, using the Analysis of Functional NeuroImages program 3dClustSim.

rCBF, regional cerebral blood flow.

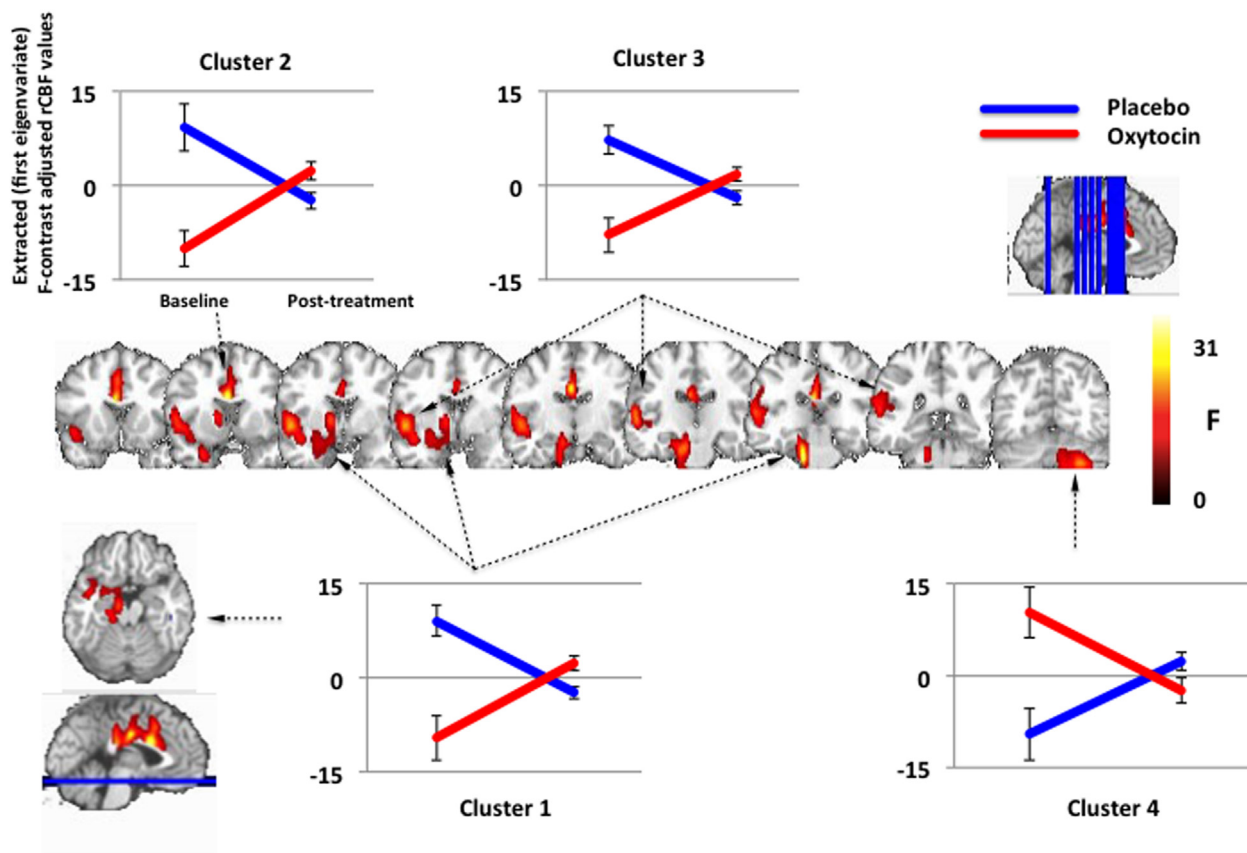


Figure 3. Statistical parametric maps for the four clusters showing a significant Treatment (intranasal oxytocin [$n = 16$], placebo [$n = 16$]) \times Period (baseline, after administration) interaction (F contrast) over the entire observation interval of 25–78 minutes following the onset of treatment. Inserted graphs plot the extracted (first eigenvariate), F contrast adjusted rCBF values for each cluster to illustrate the interaction effect. Error bars represent SE. The right-hand side of each image corresponds to the participant's right side. Slice numbers indicate Montreal Neurological Institute coordinates. rCBF, regional cerebral blood flow.

after the onset of IN-OT administration and were consistent with a pharmacodynamic profile showing a peak response at 39–51 minutes, followed by a gradual diminution of effects.

Mapping the Oxytocinergic Network in the Human Brain

The significant Treatment \times Period crossover interaction identified cortical and subcortical regions showing higher rCBF after treatment in the IN-OT group compared with the placebo group, controlling for baseline differences. Most of the subcortical limbic areas and the anterior cingulate gyrus have been previously reported to express OT receptors in post-mortem human brains (33–35). In the rat, OT receptors were also identified in insular and temporal lobe regions (62,77), but no evidence exists for humans.

The brain areas showing increased rCBF following IN-OT at rest are part of a distributed “social brain” network (56–58,78–84) (see the *Supplement* for a discussion of findings in relation to the role of OT in centrally mediated physiologic functions). This network underpins the processing of social and emotional stimuli and the expression of social and affiliative behavior (85–88). For example, it involves subcircuits such as the human mirror system (80,82), those involved in cognitive and emotional

empathy (78,79,81,83,84) or theory of mind and mentalizing (89) (*Supplement*). Neural activity in this network is consistently modulated by an acute dose of IN-OT during social tasks (10,39,90–102) and has been linked to differences in peripheral OT levels (103). A meta-analysis of studies involving the processing of emotional stimuli showed that IN-OT increased BOLD signal over a single cluster centered on the left insula, extending into the superior temporal and paracentral gyri (104). Additionally, IN-OT enhanced neural activity within the oxytocinergic network in children with autism spectrum disorder while making social judgments (23). A single IN-OT dose (compared with placebo) also modulates functional connectivity between nodes of the oxytocinergic network when participants engage in tasks requiring social cognitive or emotional processing (10,90–102) or are at rest (39). For example, Striepens *et al.* (105) reported that IN-OT (compared with placebo) enhanced functional connectivity among the left amygdala, left anterior insula, and left inferior frontal gyrus, whereas Riem *et al.* (40) reported increased functional connectivity among the cingulate and somatosensory cortices and the cerebellum.

The reverse pattern was shown by rCBF changes in the right posterior cerebellar lobules: rCBF decreased after IN-OT treatment compared with placebo. These cerebellar lobules

Table 2. Performance Parameters for the Gaussian Process Classification Model

Contrast	Accuracy	p^a	Sensitivity	Specificity	Predictive p (Postnasal Spray rCBF Map)
			(%)	(%)	(M \pm SE)
Post IN-OT Class					
25–38 min	.83	<.001	81.25	81.25	.69 \pm .05
32–44 min	.83	<.001	81.25	81.25	.73 \pm .05
39–51 min	.94	<.001	93.75	93.75	.80 \pm .03
45–58 min	1.00	<.001	100.00	100.00	.77 \pm .03
52–65 min	.88	<.001	87.5	87.5	.73 \pm .04
59–71 min	.88	<.001	87.5	87.5	.71 \pm .05
66–78 min	.83	<.001	81.25	81.25	.70 \pm .05
Post Placebo Class					
25–38 min	.69	>.05	68.75	68.75	.64 \pm .05
32–44 min	.81	<.001	81.25	81.25	.66 \pm .05
39–51 min	.63	>.05	62.5	62.5	.62 \pm .05
45–58 min	.69	>.05	68.75	68.75	.58 \pm .05
52–65 min	.38	>.05	37.5	37.5	.55 \pm .05
59–71 min	.56	>.05	56.25	56.25	.59 \pm .05
66–78 min	.63	>.05	62.5	62.5	.61 \pm .05

Performance of the Gaussian process classification was assessed using the leave-one-out procedure; statistical significance of the classification accuracies was determined by random permutation and adjusted for multiple testing using the Holm-Bonferroni correction procedure.

IN-OT, intranasal oxytocin; rCBF, regional cerebral blood flow.

^aHolm-Bonferroni corrected values.

show strong functional connections with cerebral limbic association networks and networks related to executive control (106). This right laterality is consistent with the predominantly contralateral cerebral-cerebellar mappings (106,107) and the notable asymmetry in functional specialization in the cerebellum (108). A low OT concentration (109) and the projection of afferent OT fibers (62) in the cerebellum have been reported in rats, but there is currently no evidence in humans. However, the cerebellum is increasingly being recognized to play an important role in aspects of social cognition requiring high levels of abstraction in humans (110). This role is consistent with the presence of anatomic and functional cerebellar abnormalities in autistic spectrum disorders in which social dysfunction is one of the core symptoms (111). Further studies are required to elucidate the exact causes of the observed IN-OT effects in rCBF in the cerebellum.

Changes in rCBF at rest induced by IN-OT showed a predominantly left hemisphere laterality (and consistently with a contralateral cerebral-cerebellar mapping, the right cerebellum). This finding is remarkably consistent with the meta-analytic evidence that IN-OT modulated activity over a specifically left hemisphere network during processing of emotional stimuli (104). These regions were also part of the maternal brain network responding to visual or auditory stimuli of the mother's own (compared with unknown) children (104). The mammalian brain, from humans to mice, shows a left hemisphere advantage in processing species-specific communication sounds (112). Resting-state fMRI and task-based studies have also reported hemispheric asymmetries regarding the modulatory effects of

IN-OT on amygdala functional connectivity (105) or amygdala response involving left (92,98,113,114) or right amygdala laterality (97,100,101). These findings might be consistent with the noted functional asymmetry in the amygdala, with right amygdala involved in the rapid, automatic recognition of threatening stimuli and left amygdala involved in the conscious perception and regulation of the level of the emotional response (115). The reported effects of IN-OT in left amygdala in the resting state may relate to the anxiolytic effects of IN-OT in humans (116). A similar left hemisphere laterality has been reported regarding IN-OT modulatory effects in the striatum and frontal and temporal cortex regions (92,98,113,114), and several nodes in the social brain network [e.g., inferior parietal cortex (117) or inferior frontal gyrus (74,118)]. The left hemisphere bias regarding IN-OT effects on brain function might reflect the known lateralization of key cognitive processes required for life in large social networks, such as communication skills and group membership categorization, to the left hemisphere (119).

Existing histologic evidence from postmortem human brains cannot illuminate the observed asymmetries in the functional effects of IN-OT. Early studies did not report the hemispheric origin of their samples (33,34); a later study included some bilateral but mostly left hemisphere samples (35). Genetic imaging studies that investigate the effects of polymorphic variation in the OT receptor gene on brain structure (120–124) and function (122,123,125–130) might shed further light. However, to date, there are too few studies and too great a range of tasks for a consistent pattern to emerge. Overall, these studies involve the same cortical and subcortical regions composing the oxytocinergic network identified here, including bilateral (e.g., anterior cingulate cortex) (123,127) or predominantly left hemisphere (122,125,126,128,130) and right cerebellum effects (Supplement) (127).

Table 3. Treatment \times Period ANOVA on Predictive Probabilities Computed Using Gaussian Process Classification on rCBF Maps

	χ^2a	df ^a	p
Predictive Probabilities			
Treatment	5.43	1	.02
Period	7.34	6	.29
Treatment \times Period	13.59	6	.035
Simple Effects Analyses ^b			
Treatment effect at 25–38 min	.49	1	.49
Treatment effect at 32–44 min	.94	1	.66
Treatment effect at 39–51 min	8.81	1	.018
Treatment effect at 45–58 min	9.98	1	.011
Treatment effect at 52–65 min	6.97	1	.042
Treatment effect at 59–71 min	3.44	1	.25
Treatment effect at 66–78 min	1.69	1	.58
Period effect in IN-OT group	15.06	6	.040
Period effect in placebo group	10.16	6	.12

ANOVA, analysis of variance; IN-OT, intranasal oxytocin; rCBF, regional cerebral blood flow.

^aThe bootstrap procedure in Stata uses χ^2 statistics to test for statistical significance, which we report (equivalent F values can be obtained by dividing the χ^2 statistic by its degrees of freedom).

^bReported p values are adjusted for multiple testing using the sequential Holm-Bonferroni correction procedure.

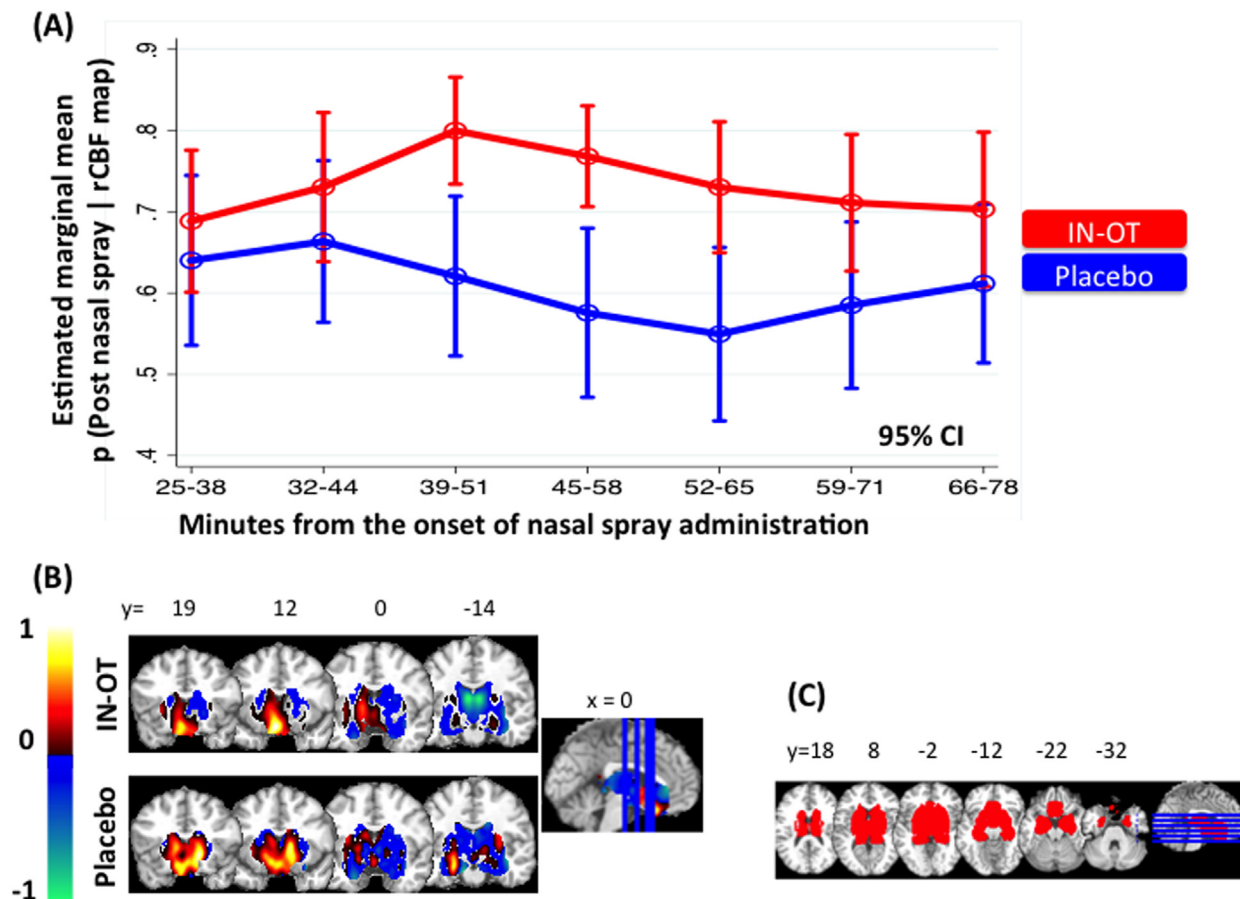


Figure 4. Pattern recognition analyses. **(A)** Estimated marginal mean predictive probabilities for the post nasal spray administration class (y axis) (and 95% confidence intervals) for the Treatment (IN-OT [$n = 16$], placebo [$n = 16$]) \times Period (baseline, after administration) interaction as a function of time interval, using an a priori defined mask of brain regions likely to express oxytocin receptors. Note the temporal overlap between adjacent time intervals; to sample the entire postoxytocin period, we averaged all pairs of adjacent regional cerebral blood flow maps. We observed a significant main effect for Treatment [$\chi^2_1 = 5.43, p = .020$], but not for Period [$\chi^2_6 = 7.34, p = .29$], and a significant Treatment \times Period interaction [$\chi^2_6 = 13.59, p = .035$] (corrected p values reported). The mean predictive probabilities for the post-IN-OTclass followed a pharmacodynamic profile showing a peak response at 39–51 minutes, followed by a gradual diminution of effects. **(B)** Multivariate maps of normalized weight vectors from the Gaussian process classification (g-maps) at the 39–51 minute interval that contrast the post-IN-OT/placebo classes to the baseline class. Positive coefficients (red color scale) indicate a positive contribution to the prediction for each class, and negative coefficients (blue color scale) indicate a negative contribution. A positive g-map coefficient for a particular voxel indicates a higher overall β weight for the post-IN-OT/placebo class, and similarly a negative g-map coefficient indicates a higher overall β score for the baseline class. A region with a high weight cannot be interpreted as driving the classification; the whole pattern of weights drives the classification. These maps cannot be used to make inferences about local activation. The right-hand side of each image corresponds to the participant's right side. Slice numbers indicate Montreal Neurological Institute coordinates. **(C)** The a priori defined mask of brain regions likely to express oxytocin receptors included the subcallosal area (including basal forebrain regions), nucleus accumbens, caudate nucleus, putamen, globus pallidus, amygdala, hippocampus, thalamus, and hypothalamus. The hypothalamus was defined with a sphere centered on Montreal Neurological Institute coordinates ($x y z: 0, -4, -8$) using a 12-mm radius (146,147). The remaining regions of interest were defined using the Harvard-Oxford cortical and subcortical structural atlases in FSLview (<http://fsl.fmrib.ox.ac.uk>). CI, confidence interval; IN-OT, intranasal oxytocin; rCBF, regional cerebral blood flow.

Ascertaining Temporal Dynamics of IN-OT Effects on Human Brain Physiology

The application of GPC on rCBF maps reflecting the distributed effects of IN-OT or placebo yielded two main findings. First, classification accuracies were significant for scans after administration compared with baseline scans at all temporal intervals for the IN-OT group, but not the placebo group: predictive probabilities for the former were significantly higher than predictive probabilities for the latter. This finding suggests that IN-OT-induced changes in rCBF—and hence

neuronal metabolism (131) and activity (50–53,55)—were sustained over the entire observation interval.

Physiologically, this finding is consistent with evidence from animal studies that endogenous or exogenous OT binds on hypothalamic OT-secreting neurons initiating energy-demanding processes that induce prolonged effects on physiology and behavior that last >1 hour (28,29,132,133). Human studies provide indirect support: an acute dose of IN-OT (compared with placebo) leads to an elevated concentration of OT in the CSF at 75 minutes in adult male volunteers (30) and for 7 hours after administration in saliva (134,135),

possibly by engaging hypothalamic OT neurons in a feed-forward loop. However, the peripheral and central release of OT are dissociated (28); plasma and CSF OT levels do not correlate in humans (136–139), and peripheral OT cannot cross the blood-brain barrier in sufficient quantities to induce central changes (140). Our findings suggest that changes in rCBF provide a quantifiable, reliable index to link peripheral changes in OT concentration with central effects following IN-OT.

Our second finding was that the temporal profile of IN-OT-induced rCBF changes showed a peak response 39–51 minutes after IN-OT, followed by a gradual diminution of effects. This finding matches the slow pharmacokinetics of OT in the CSF (141) and is remarkably consistent with the dynamic changes in OT concentration in the extracellular fluid in the amygdala and hippocampi in rodents that peaked 30–60 minutes after the intranasal application of OT (31). The release of endogenous OT also shows a similar pattern in rodents when triggered with alpha-melanocyte-stimulating hormone, peaking ~20–30 minutes after stimulation (133).

Limitations

Using independent groups for the IN-OT and placebo arms and concealing the identity of the nasal spray until debriefing offered protection against OT-related expectation effects (e.g., as might have arisen from differential exposure to media hype about expected outcomes of OT). In a crossover design, the absence of perceivable changes in subjective experience following IN-OT (66) might have led participants to think that they had received placebo. However, our independent groups design may have inflated the between-subject variance, which precluded cross-group PR. Given the nature of this study, conducted at rest and by treatment-naïve radiographers, with minimal interaction between the main investigator and participants, a single-blind design (where the main investigator was not naïve regarding the administered compound) was deemed sufficient. Finally, we focused on male participants because some degree of sexual dimorphism in the OT system (92,97,142) may be expected, and most participants in experimental studies (66) and clinical trials [e.g., in autistic spectrum disorders (19–23,25)] are male, aiming to maximize the applicability and resource efficiency for this novel study. Our findings need to be replicated in a double-blinded, crossover design including both genders.

Conclusions

Our findings are consistent with animal evidence and extend this evidence to humans. Our findings provide the experimenter and clinician with direct evidence to guide decision making, guide research in the pharmacokinetics and pharmacodynamics of IN-OT, and inform the development of theoretical and mechanistic accounts regarding effects of OT on typical and atypical social behavior. The power of arterial spin labeling to quantify the effects of IN-OT on brain physiology renders it a promising, noninvasive, *in vivo* method to investigate the impact of genetic (9,143), epigenetic (126), social-environmental (40), and contextual (144) factors on the baseline function of the OT system. Additionally, the quantification of IN-OT effects on brain physiology will allow the establishment of dose-response associations between achieved effects on neurophysiology and behavior or clinical symptoms. This information will contribute

to enhancing the validity and reliability of clinical trials investigating the therapeutic potential of IN-OT and cannot be obtained using the nominal dosage of extant nasal sprays because it does not reliably reflect tissue absorption (145).

ACKNOWLEDGMENTS AND DISCLOSURES

This work was supported by Economic and Social Research Council fellowship Grant No. ES/K009400/1 (to YP), the Volkswagen Foundation “European Platform for Life Sciences, Mind Sciences and Humanities” Grant No. II/85 069 (to AF), Institute for the Study of Affective Neuroscience/Hope for Depression Research Foundation (to AF), European Research Council Starting Investigator Award Grant No. ERC-2012-STG GA313755 (to AF), Innovative Medicines Initiative Joint Undertaking under Grant Agreement No. 115008 (NEWMEDS consortium) (to OMD), and Medical Research Council Developmental Pathway Funding Scheme Grant No. MR/J005142/1 (to MAH and SCW). The Innovative Medicines Initiative Joint Undertaking is a public-private partnership between the European Union and the European Federation of Pharmaceutical Industries and Associations.

We thank our participants and Dr. D. Alsop for facilitating the pulsed-continuous arterial spin labeling pulse sequence used in this work. We also thank the National Institute for Health Research, Biomedical Research Centre for Mental Health at South London and Maudsley National Health Service Foundation Trust and Institute of Psychiatry, King’s College London for their continued infrastructure support of our neuroimaging research.

The authors report no biomedical financial interests or potential conflicts of interest.

ARTICLE INFORMATION

From the Department of Neuroimaging (YP, OMD, FOZ, SCW, MAH), Institute of Psychiatry, King’s College London, London; Department of Forensic and Neurodevelopmental Science (SM), Institute of Psychiatry, King’s College London, London; and Research Department of Clinical, Educational, and Health Psychology (AF), University College London, London, United Kingdom.

AF and MAH are joint senior authors.

Address correspondence to Yannis Paloyelis, Ph.D., Department of Neuroimaging, Institute of Psychiatry, King’s College London, De Crespigny Park Road, London SE5 8AF, UK; E-mail: Yannis.Paloyelis@kcl.ac.uk.

Received May 14, 2014; revised Aug 21, 2014; accepted Oct 7, 2014.

Supplementary material cited in this article is available online at <http://dx.doi.org/10.1016/j.biopsych.2014.10.005>.

REFERENCES

- Donaldson ZR, Young LJ (2008): Oxytocin, vasopressin, and the neurogenetics of sociality. *Science* 322:900–904.
- Insel TR (2010): The challenge of translation in social neuroscience: A review of oxytocin, vasopressin, and affiliative behavior. *Neuron* 65:768–779.
- Nelson E, Panksepp J (1996): Oxytocin mediates acquisition of maternally associated odor preferences in preweanling rat pups. *Behav Neurosci* 110:583–592.
- Takayanagi Y, Yoshida M, Bielsky IF, Ross HE, Kawamata M, Onaka T, et al. (2005): Pervasive social deficits, but normal parturition, in oxytocin receptor-deficient mice. *Proc Natl Acad Sci U S A* 102:16096–16101.
- Williams JR, Insel TR, Harbaugh CR, Carter CS (1994): Oxytocin administered centrally facilitates formation of a partner preference in female prairie voles (*Microtus ochrogaster*). *J Neuroendocrinol* 6: 247–250.
- Ross HE, Freeman SM, Spiegel LL, Ren X, Terwilliger EF, Young LJ (2009): Variation in oxytocin receptor density in the nucleus accumbens has differential effects on affiliative behaviors in monogamous and polygamous voles. *J Neurosci* 29:1312–1318.
- Ferguson JN, Aldag JM, Insel TR, Young LJ (2001): Oxytocin in the medial amygdala is essential for social recognition in the mouse. *J Neurosci* 21:8278–8285.

8. Landgraf R, Neumann ID (2004): Vasopressin and oxytocin release within the brain: A dynamic concept of multiple and variable modes of neuropeptide communication. *Front Neuroendocrinol* 25:150–176.
9. Skuse DH, Lori A, Cubells JF, Lee I, Conneely KN, Puura K, et al. (2014): Common polymorphism in the oxytocin receptor gene (OXTR) is associated with human social recognition skills. *Proc Natl Acad Sci U S A* 111:1987–1992.
10. Meyer-Lindenberg A, Domes G, Kirsch P, Heinrichs M (2011): Oxytocin and vasopressin in the human brain: Social neuropeptides for translational medicine. *Nat Rev Neurosci* 12:524–538.
11. Zink CF, Meyer-Lindenberg A (2012): Human neuroimaging of oxytocin and vasopressin in social cognition. *Horm Behav* 61:400–409.
12. Macdonald K, Macdonald TM (2010): The peptide that binds: A systematic review of oxytocin and its prosocial effects in humans. *Harv Rev Psychiatry* 18:1–21.
13. Guastella AJ, MacLeod C (2012): A critical review of the influence of oxytocin nasal spray on social cognition in humans: Evidence and future directions. *Horm Behav* 61:410–418.
14. Grillon C, Krinsky M, Charney DR, Vytal K, Ernst M, Cornwell B (2013): Oxytocin increases anxiety to unpredictable threat. *Mol Psychiatry* 18:958–960.
15. MacDonald K, MacDonald TM, Brune M, Lamb K, Wilson MP, Golshan S, et al. (2013): Oxytocin and psychotherapy: A pilot study of its physiological, behavioral and subjective effects in males with depression. *Psychoneuroendocrinology* 38:2831–2843.
16. Shalvi S, De Dreu CKW (2014): Oxytocin promotes group-serving dishonesty. *Proc Natl Acad Sci U S A* 111:5503–5507.
17. Van IMH, Bakermans-Kranenburg MJ (2012): A sniff of trust: Meta-analysis of the effects of intranasal oxytocin administration on face recognition, trust to in-group, and trust to out-group, *Psychoneuroendocrinology* 37:438–443.
18. Young LJ (2013): When too much of a good thing is bad: Chronic oxytocin, development, and social impairments. *Biol Psychiatry* 74: 160–161.
19. Anagnostou E, Soorya L, Chaplin W, Bartz J, Halpern D, Wasserman S, et al. (2012): Intranasal oxytocin versus placebo in the treatment of adults with autism spectrum disorders: A randomized controlled trial. *Mol Autism* 3:16.
20. Andari E, Duhamel JR, Zalla T, Herbrecht E, Leboyer M, Sirigu A (2010): Promoting social behavior with oxytocin in high-functioning autism spectrum disorders. *Proc Natl Acad Sci U S A* 107: 4389–4394.
21. Dadds MR, MacDonald E, Cauchi A, Williams K, Levy F, Brennan J (2014): Nasal oxytocin for social deficits in childhood autism: A randomized controlled trial. *J Autism Dev Disord* 44:521–531.
22. Domes G, Heinrichs M, Kumbier E, Grossmann A, Hauenstein K, Herpertz SC (2013): Effects of intranasal oxytocin on the neural basis of face processing in autism spectrum disorder. *Biol Psychiatry* 74: 164–171.
23. Gordon I, Vander Wyk BC, Bennett RH, Cordeaux C, Lucas MV, Eiblott JA, et al. (2013): Oxytocin enhances brain function in children with autism. *Proc Natl Acad Sci U S A* 110:20953–20958.
24. Kim YR, Kim CH, Park JH, Pyo J, Treasure J (2014): The impact of intranasal oxytocin on attention to social emotional stimuli in patients with anorexia nervosa: A double blind within-subject cross-over experiment. *PloS One* 9:e90721.
25. Lin IF, Kashino M, Ohta H, Yamada T, Tani M, Watanabe H, et al. (2014): The effect of intranasal oxytocin versus placebo treatment on the autonomic responses to human sounds in autism: A single-blind, randomized, placebo-controlled, crossover design study. *Mol Autism* 5:20.
26. Bakermans-Kranenburg MJ, van IJMH (2013): Sniffing around oxytocin: Review and meta-analyses of trials in healthy and clinical groups with implications for pharmacotherapy. *Transl Psychiatry* 3:e258.
27. Born J, Lange T, Kern W, McGregor GP, Bickel U, Fehm HL (2002): Sniffing neuropeptides: A transnasal approach to the human brain. *Nat Neurosci* 5:514–516.
28. Ludwig M, Leng G (2006): Dendritic peptide release and peptide-dependent behaviours. *Nat Rev Neurosci* 7:126–136.
29. Stoop R (2012): Neuromodulation by oxytocin and vasopressin. *Neuron* 76:142–159.
30. Striepens N, Kendrick KM, Hanking V, Landgraf R, Wullner U, Maier W, et al. (2013): Elevated cerebrospinal fluid and blood concentrations of oxytocin following its intranasal administration in humans. *Sci Rep* 3:3440.
31. Neumann ID, Maloumby R, Beiderbeck DI, Lukas M, Landgraf R (2013): Increased brain and plasma oxytocin after nasal and peripheral administration in rats and mice. *Psychoneuroendocrinology* 38:1985–1993.
32. Insel TR, Young LJ (2001): The neurobiology of attachment. *Nat Rev Neurosci* 2:129–136.
33. Loup F, Tribollet E, Dubois-Dauphin M, Dreifuss JJ (1991): Localization of high-affinity binding sites for oxytocin and vasopressin in the human brain. An autoradiographic study. *Brain Res* 555:220–232.
34. Loup F, Tribollet E, Dubois-Dauphin M, Pizzolato G, Dreifuss JJ (1989): Localization of oxytocin binding sites in the human brainstem and upper spinal cord: An autoradiographic study. *Brain Res* 500:223–230.
35. Boccia ML, Petrusz P, Suzuki K, Marson L, Pedersen CA (2013): Immunohistochemical localization of oxytocin receptors in human brain. *Neuroscience* 253:155–164.
36. Manning M, Misicka A, Olma A, Bankowski K, Stoev S, Chini B, et al. (2012): Oxytocin and vasopressin agonists and antagonists as research tools and potential therapeutics. *J Neuroendocrinol* 24:609–628.
37. Chen Y, Wan HI, O'Reardon JP, Wang DJ, Wang Z, Korczynski M, et al. (2011): Quantification of cerebral blood flow as biomarker of drug effect: Arterial spin labeling phMRI after a single dose of oral citalopram. *Clin Pharmacol Ther* 89:251–258.
38. Zelaya FO, Zois E, Muller-Pollard C, Lythgoe DJ, Lee S, Andrews C, et al. (2012): The response to rapid infusion of fentanyl in the human brain measured using pulsed arterial spin labelling. *Magma* 25: 163–175.
39. Sripada CS, Phan KL, Labuschagne I, Welsh R, Nathan PJ, Wood AG (2013): Oxytocin enhances resting-state connectivity between amygdala and medial frontal cortex. *Int J Neuropsychopharmacol* 16:255–260.
40. Riem MM, van IJzendoorn MH, Tops M, Boksem MA, Rombouts SA, Bakermans-Kranenburg MJ (2013): Oxytocin effects on complex brain networks are moderated by experiences of maternal love withdrawal. *Eur Neuropsychopharmacol* 23:1288–1295.
41. Detre JA, Leigh JS, Williams DS, Koretsky AP (1992): Perfusion imaging. *Magn Reson Med* 23:37–45.
42. Williams DS, Detre JA, Leigh JS, Koretsky AP (1992): Magnetic resonance imaging of perfusion using spin inversion of arterial water. *Proc Natl Acad Sci U S A* 89:212–216.
43. Handley R, Zelaya FO, Reinders AA, Marques TR, Mehta MA, O'Gorman R, et al. (2013): Acute effects of single-dose aripiprazole and haloperidol on resting cerebral blood flow (rCBF) in the human brain. *Hum Brain Mapp* 34:272–282.
44. Doyle OM, De Simoni S, Schwarz AJ, Brittain C, O'Daly OG, Williams SC, et al. (2013): Quantifying the attenuation of the ketamine pharmacological magnetic resonance imaging response in humans: A validation using antipsychotic and glutamatergic agents. *J Pharmacol Exp Ther* 345:151–160.
45. Marquand AF, O'Daly OG, De Simoni S, Alsop DC, Maguire RP, Williams SC, et al. (2012): Dissociable effects of methylphenidate, atomoxetine and placebo on regional cerebral blood flow in healthy volunteers at rest: A multi-class pattern recognition approach. *Neuroimage* 60:1015–1024.
46. Viviani R, Abler B, Seeringer A, Stingl JC (2012): Effect of paroxetine and bupropion on human resting brain perfusion: An arterial spin labeling study. *Neuroimage* 61:773–779.
47. Nordin LE, Li TQ, Brogren J, Johansson P, Sjogren N, Hannesson K, et al. (2013): Cortical responses to amphetamine exposure studied by pCASL MRI and pharmacokinetic/pharmacodynamic dose modeling. *Neuroimage* 68:75–82.
48. Wang DJ, Chen Y, Fernandez-Seara MA, Detre JA (2011): Potentials and challenges for arterial spin labeling in pharmacological magnetic resonance imaging. *J Pharmacol Exp Ther* 337:359–366.

49. Hodkinson DJ, Krause K, Khawaja N, Renton TF, Huggins JP, Vennart W, et al. (2013): Quantifying the test-retest reliability of cerebral blood flow measurements in a clinical model of on-going post-surgical pain: A study using pseudo-continuous arterial spin labelling. *Neuroimage Clin* 3:301–310.
50. Attwell D, Buchan AM, Charpak S, Lauritzen M, Macvicar BA, Newman EA (2010): Glial and neuronal control of brain blood flow. *Nature* 468:232–243.
51. Sokoloff L (1981): Relationships among local functional activity, energy metabolism, and blood flow in the central nervous system. *Fed Proc* 40:2311–2316.
52. Raichle ME, Grubb RL Jr, Gado MH, Eichling JO, Ter-Pogossian MM (1976): Correlation between regional cerebral blood flow and oxidative metabolism. In vivo studies in man. *Arch Neurol* 33:523–526.
53. Roland PE, Eriksson L, Stone-Elander S, Widen L (1987): Does mental activity change the oxidative metabolism of the brain? *J Neurosci* 7:2373–2389.
54. Tsubokawa T, Katayama Y, Kondo T, Ueno Y, Hayashi N, Moriyasu N (1980): Changes in local cerebral blood flow and neuronal activity during sensory stimulation in normal and sympathectomized cats. *Brain Res* 190:51–64.
55. Hirano Y, Stefanovic B, Silva AC (2011): Spatiotemporal evolution of the functional magnetic resonance imaging response to ultrashort stimuli. *J Neurosci* 31:1440–1447.
56. Adolphs R (2001): The neurobiology of social cognition. *Curr Opin Neurobiol* 11:231–239.
57. Adolphs R (2009): The social brain: Neural basis of social knowledge. *Annu Rev Psychol* 60:693–716.
58. Amadio DM, Frith CD (2006): Meeting of minds: The medial frontal cortex and social cognition. *Nat Rev Neurosci* 7:268–277.
59. Lowbridge J, Manning M, Halder J, Sawyer WH (1977): Synthesis and some pharmacological properties of [4-threonine, 7-glycine] oxytocin, [1-(L-2-hydroxy-3-mercaptopropanoic acid), 4-threonine, 7-glycine]oxytocin (hydroxy[Thr4, Gly7]oxytocin), and [7-glycine]oxytocin, peptides with high oxytocin-antidiuretic selectivity. *J Med Chem* 20:120–123.
60. Norman KA, Polyn SM, Detre GJ, Haxby JV (2006): Beyond mind-reading: Multi-voxel pattern analysis of fMRI data. *Trends Cogn Sci* 10:424–430.
61. Doyle OM, Ashburner J, Zelaya FO, Williams SC, Mehta MA, Marquand AF (2013): Multivariate decoding of brain images using ordinal regression. *Neuroimage* 81:347–357.
62. Gimpl G, Fahrenholz F (2001): The oxytocin receptor system: Structure, function, and regulation. *Physiol Rev* 81:629–683.
63. Murphy K, Harris AD, Diukova A, Evans CJ, Lythgoe DJ, Zelaya F, et al. (2011): Pulsed arterial spin labeling perfusion imaging at 3 T: Estimating the number of subjects required in common designs of clinical trials. *Magn Reson Imaging* 29:1382–1389.
64. Derogatis LR, Savitz KL (2000): The SCL-90-R and the Brief Symptom Inventory (BSI) in primary care. In: Maruish ME, editor. *Handbook of Psychological Assessment in Primary Care Settings*. Mahwah, NJ: Lawrence Erlbaum Associates, 297–334.
65. Beck AT, Steer RA, Ball R, Ranieri W (1996): Comparison of Beck Depression Inventories -IA and -II in psychiatric outpatients. *J Pers Assess* 67:588–597.
66. MacDonald E, Dadds MR, Brennan JL, Williams K, Levy F, Cauchi AJ (2011): A review of safety, side-effects and subjective reactions to intranasal oxytocin in human research. *Psychoneuroendocrinology* 36:1114–1126.
67. Dai W, Garcia D, de Bazelaire C, Alsop DC (2008): Continuous flow-driven inversion for arterial spin labeling using pulsed radio frequency and gradient fields. *Magn Reson Med* 60:1488–1497.
68. Cuzick J (1985): A Wilcoxon-type test for trend. *Stat Med* 4:87–90.
69. Williams RL (2000): A note on robust variance estimation for cluster-correlated data. *Biometrics* 56:645–646.
70. Holm S (1979): A simple sequentially rejective multiple test procedure. *Scand J Stat* 6:65–70.
71. Vickers AJ, Altman DG (2001): Statistics notes: Analysing controlled trials with baseline and follow up measurements. *BMJ* 323:1123–1124.
72. Worsley KJ (2001): Statistical analysis of activation images. In: Jezzard P, Matthews PM, Smith SM, editors. *Functional MRI: An Introduction to Methods*. Oxford: OUP.
73. Rasmussen CE, Williams CKI (2006): *Gaussian Processes for Machine Learning*. Cambridge: MIT Press.
74. Mars RB, Neubert FX, Noonan MP, Sallet J, Toni I, Rushworth MF (2012): On the relationship between the “default mode network” and the “social brain”. *Front Hum Neurosci* 6:189.
75. Van Overwalle F (2009): Social cognition and the brain: A meta-analysis. *Hum Brain Mapp* 30:829–858.
76. Kennedy DP, Adolphs R (2012): The social brain in psychiatric and neurological disorders. *Trends Cogn Sci* 16:559–572.
77. Ophir AG, Gessel A, Zheng DJ, Phelps SM (2012): Oxytocin receptor density is associated with male mating tactics and social monogamy. *Horm Behav* 61:445–453.
78. Fan Y, Duncan NW, de Groot M, Northoff G (2011): Is there a core neural network in empathy? An fMRI based quantitative meta-analysis. *Neurosci Biobehav Rev* 35:903–911.
79. Carr L, Iacoboni M, Dubeau MC, Mazziotta JC, Lenzi GL (2003): Neural mechanisms of empathy in humans: A relay from neural systems for imitation to limbic areas. *Proc Natl Acad Sci U S A* 100:5497–5502.
80. Hall J, Philip RC, Marwick K, Whalley HC, Romaniuk L, McIntosh AM, et al. (2012): Social cognition, the male brain and the autism spectrum. *PLoS One* 7:e49033.
81. Iacoboni M (2009): Imitation, empathy, and mirror neurons. *Annu Rev Psychol* 60:653–670.
82. Russell TA, Rubia K, Bullmore ET, Soni W, Suckling J, Brammer MJ, et al. (2000): Exploring the social brain in schizophrenia: Left prefrontal underactivation during mental state attribution. *Am J Psychiatry* 157:2040–2042.
83. Shamay-Tsoory SG, Aharon-Peretz J, Perry D (2009): Two systems for empathy: A double dissociation between emotional and cognitive empathy in inferior frontal gyrus versus ventromedial prefrontal lesions. *Brain* 132:617–627.
84. Shamay-Tsoory SG, Fischer M, Dvash J, Harari H, Perach-Bloom N, Levkovitz Y (2009): Intranasal administration of oxytocin increases envy and schadenfreude (gloating). *Biol Psychiatry* 66:864–870.
85. Pessoa L, Adolphs R (2010): Emotion processing and the amygdala: From a ‘low road’ to ‘many roads’ of evaluating biological significance. *Nat Rev Neurosci* 11:773–783.
86. Tsuchiya N, Moradi F, Felsen C, Yamazaki M, Adolphs R (2009): Intact rapid detection of fearful faces in the absence of the amygdala. *Nat Neurosci* 12:1224–1225.
87. Kennedy DP, Glascher J, Tyszka JM, Adolphs R (2009): Personal space regulation by the human amygdala. *Nat Neurosci* 12:1226–1227.
88. Adolphs R, Tranel D, Damasio AR (1998): The human amygdala in social judgment. *Nature* 393:470–474.
89. Hillis AE (2014): Inability to empathize: Brain lesions that disrupt sharing and understanding another’s emotions. *Brain* 137(pt 4):981–997.
90. Baumgartner T, Heinrichs M, Vonlanthen A, Fischbacher U, Fehr E (2008): Oxytocin shapes the neural circuitry of trust and trust adaptation in humans. *Neuron* 58:639–650.
91. Domes G, Heinrichs M, Michel A, Berger C, Herpertz SC (2007): Oxytocin improves “mind-reading” in humans. *Biol Psychiatry* 61:731–733.
92. Domes G, Lischke A, Berger C, Grossmann A, Hauenstein K, Heinrichs M, et al. (2010): Effects of intranasal oxytocin on emotional face processing in women. *Psychoneuroendocrinology* 35:83–93.
93. Gamer M (2010): Does the amygdala mediate oxytocin effects on socially reinforced learning? *J Neurosci* 30:9347–9348.
94. Labuschagne I, Phan KL, Wood A, Angstadt M, Chua P, Heinrichs M, et al. (2010): Oxytocin attenuates amygdala reactivity to fear in generalized social anxiety disorder. *Neuropsychopharmacology* 35:2403–2413.
95. Labuschagne I, Phan KL, Wood A, Angstadt M, Chua P, Heinrichs M, et al. (2011): Medial frontal hyperactivity to sad faces in

- generalized social anxiety disorder and modulation by oxytocin. *Int J Neuropsychopharmacol* Oct 14:1–14.
96. Lischke A, Berger C, Prehn K, Heinrichs M, Herpertz SC, Domes G (2012): Intranasal oxytocin enhances emotion recognition from dynamic facial expressions and leaves eye-gaze unaffected. *Psychoneuroendocrinology* 37:475–481.
 97. Lischke A, Gamer M, Berger C, Grossmann A, Hauenstein K, Heinrichs M, et al. (2012): Oxytocin increases amygdala reactivity to threatening scenes in females. *Psychoneuroendocrinology* 37:1431–1438.
 98. Petrovic P, Kalisch R, Singer T, Dolan RJ (2008): Oxytocin attenuates affective evaluations of conditioned faces and amygdala activity. *J Neurosci* 28:6607–6615.
 99. Pincus D, Kose S, Arana A, Johnson K, Morgan PS, Borckardt J, et al. (2010): Inverse effects of oxytocin on attributing mental activity to others in depressed and healthy subjects: A double-blind placebo controlled fMRI study. *Front Psychiatry* 1:134.
 100. Riem MM, Bakermans-Kranenburg MJ, Pieper S, Tops M, Boksem MA, Vermeiren RR, et al. (2011): Oxytocin modulates amygdala, insula, and inferior frontal gyrus responses to infant crying: A randomized controlled trial. *Biol Psychiatry* 70:291–297.
 101. Riem MM, van IMH, Tops M, Boksem MA, Rombouts SA, Bakermans-Kranenburg MJ (2012): No laughing matter: Intranasal oxytocin administration changes functional brain connectivity during exposure to infant laughter. *Neuropsychopharmacology* 37:1257–1266.
 102. Schulze L, Lischke A, Greif J, Herpertz SC, Heinrichs M, Domes G (2011): Oxytocin increases recognition of masked emotional faces. *Psychoneuroendocrinology* 36:1378–1382.
 103. Atzil S, Helder T, Zagoory-Sharon O, Winetraub Y, Feldman R (2012): Synchrony and specificity in the maternal and the paternal brain: Relations to oxytocin and vasopressin. *J Am Acad Child Adolesc Psychiatry* 51:798–811.
 104. Rocchetti M, Radua J, Paloyelis Y, Xenaki LA, Frascarelli M, Caverzasi E, et al. (2014): Neurofunctional maps of the “maternal brain” and the effects of oxytocin: A multimodal voxel-based meta-analysis. *Psychiatry Clin Neurosci* 68:733–751.
 105. Striepens N, Scheele D, Kendrick KM, Becker B, Schafer L, Schwalba K, et al. (2012): Oxytocin facilitates protective responses to aversive social stimuli in males. *Proc Natl Acad Sci U S A* 109: 18144–18149.
 106. Buckner RL (2013): The cerebellum and cognitive function: 25 years of insight from anatomy and neuroimaging. *Neuron* 80:807–815.
 107. Wang D, Buckner RL, Liu H (2013): Cerebellar asymmetry and its relation to cerebral asymmetry estimated by intrinsic functional connectivity. *J Neurophysiol* 109:46–57.
 108. Petersen SE, Fox PT, Posner MI, Mintun M, Raichle ME (1989): Positron emission tomographic studies of the processing of single words. *J Cogn Neurosci* 1:153–170.
 109. Hashimoto H, Fukui K, Noto T, Nakajima T, Kato N (1985): Distribution of vasopressin and oxytocin in rat brain. *Endocrinol Jpn* 32:89–97.
 110. Van Overwalle F, Baetens K, Marien P, Vandekerckhove M (2014): Social cognition and the cerebellum: A meta-analysis of over 350 fMRI studies. *Neuroimage* 86:554–572.
 111. Fatemi SH, Aldinger KA, Ashwood P, Bauman ML, Blaha CD, Blatt GJ, et al. (2012): Consensus paper: Pathological role of the cerebellum in autism. *Cerebellum* 11:777–807.
 112. Geissler DB, Ehret G (2004): Auditory perception vs. recognition: Representation of complex communication sounds in the mouse auditory cortical fields. *Eur J Neurosci* 19:1027–1040.
 113. Rilling JK, DeMarco AC, Hackett PD, Thompson R, Ditzen B, Patel R, et al. (2012): Effects of intranasal oxytocin and vasopressin on cooperative behavior and associated brain activity in men. *Psychoneuroendocrinology* 37:447–461.
 114. Wittfoth-Schardt D, Gründing J, Wittfoth M, Lanfermann H, Heinrichs M, Domes G, et al. (2012): Oxytocin modulates neural reactivity to children’s faces as a function of social salience. *Neuropsychopharmacology* 37:1799–1807.
 115. Morris JS, Ohman A, Dolan RJ (1998): Conscious and unconscious emotional learning in the human amygdala. *Nature* 393:467–470.
 116. MacDonald K, Feifel D (2014): Oxytocin’s role in anxiety: A critical appraisal. *Brain Res* 1580:22–56.
 117. Radua J, Phillips ML, Russell T, Lawrence N, Marshall N, Kalidindi S, et al. (2010): Neural response to specific components of fearful faces in healthy and schizophrenic adults. *Neuroimage* 49:939–946.
 118. Pobric G, Hamilton AF (2006): Action understanding requires the left inferior frontal cortex. *Curr Biol* 16:524–529.
 119. Rogers LR, Vallortigara G, Andrew RJ (2013): *Divided Brains*. Cambridge: Cambridge University Press.
 120. Furman DJ, Chen MC, Gotlib IH (2011): Variant in oxytocin receptor gene is associated with amygdala volume. *Psychoneuroendocrinology* 36:891–897.
 121. Inoue H, Yamasue H, Tochigi M, Abe O, Liu X, Kawamura Y, et al. (2010): Association between the oxytocin receptor gene and amygdala volume in healthy adults. *Biol Psychiatry* 68:1066–1072.
 122. Tost H, Kolachana B, Hakimi S, Lemaire H, Verchinski BA, Mattay VS, et al. (2010): A common allele in the oxytocin receptor gene (OXTR) impacts prosocial temperament and human hypothalamic-limbic structure and function. *Proc Natl Acad Sci U S A* 107:13936–13941.
 123. Tost H, Kolachana B, Verchinski BA, Bilek E, Goldman AL, Mattay VS, et al. (2011): Neurogenetic effects of OXTR rs2254298 in the extended limbic system of healthy Caucasian adults. *Biol Psychiatry* 70:e37–e39.
 124. Yamasue H, Suga M, Yahata N, Inoue H, Tochigi M, Abe O, et al. (2011): Reply to: Neurogenetic effects of OXTR rs2254298 in the extended limbic system of healthy Caucasian adults. *Biol Psychiatry* 70:e41–e42.
 125. Damiano CR, Aloia J, Dunlap K, Burrus CJ, Mosner MG, Kozink RV, et al. (2014): Association between the oxytocin receptor (OXTR) gene and mesolimbic responses to rewards. *Mol Autism* 5:7.
 126. Jack A, Connelly JJ, Morris JP (2012): DNA methylation of the oxytocin receptor gene predicts neural response to ambiguous social stimuli. *Front Hum Neurosci* 6:280.
 127. Loth E, Poline JB, Thyreau B, Jia T, Tao C, Lourdusamy A, et al. (2014): Oxytocin receptor genotype modulates ventral striatal activity to social cues and response to stressful life events. *Biol Psychiatry* 76:367–376.
 128. Michalska KJ, Decety J, Liu C, Chen Q, Martz ME, Jacob S, et al. (2014): Genetic imaging of the association of oxytocin receptor gene (OXTR) polymorphisms with positive maternal parenting. *Front Behav Neurosci* 8:21.
 129. Montag C, Sauer C, Reuter M, Kirsch P (2013): An interaction between oxytocin and a genetic variation of the oxytocin receptor modulates amygdala activity toward direct gaze: Evidence from a pharmacological imaging genetics study. *Eur Arch Psychiatry Clin Neurosci* 263(suppl 2):S169–S175.
 130. Wang J, Qin W, Liu B, Wang D, Zhang Y, Jiang T, et al. (2013): Variant in OXTR gene and functional connectivity of the hypothalamus in normal subjects. *Neuroimage* 81:199–204.
 131. Cha YH, Jog MA, Kim YC, Chakrapani S, Kraman SM, Wang DJ (2013): Regional correlation between resting state FDG PET and pCASL perfusion MRI. *J Cereb Blood Flow Metab* 33: 1909–1914.
 132. Sabatier N, Rowe I, Leng G (2007): Central release of oxytocin and the ventromedial hypothalamus. *Biochem Soc Trans* 35: 1247–1251.
 133. Sabatier N, Caquineau C, Dayanithi G, Bull P, Douglas AJ, Guan XM, et al. (2003): Alpha-melanocyte-stimulating hormone stimulates oxytocin release from the dendrites of hypothalamic neurons while inhibiting oxytocin release from their terminals in the neurohypophysis. *J Neurosci* 23:10351–10358.
 134. van IJzendoorn MH, Bhandari R, van der Veen R, Grewen KM, Bakermans-Kranenburg MJ (2012): Elevated salivary levels of oxytocin persist more than 7 h after intranasal administration. *Front Neurosci* 6:174.
 135. Weisman O, Zagoory-Sharon O, Feldman R (2012): Intranasal oxytocin administration is reflected in human saliva. *Psychoneuroendocrinology* 37:1582–1586.
 136. Amico JA, Tenicela R, Johnston J, Robinson AG (1983): A time-dependent peak of oxytocin exists in cerebrospinal fluid but not in plasma of humans. *J Clin Endocrinol Metab* 57:947–951.

137. Jokinen J, Chatzitofis A, Hellstrom C, Nordstrom P, Uvnas-Moberg K, Asberg M (2012): Low CSF oxytocin reflects high intent in suicide attempts. *Psychoneuroendocrinology* 37:482–490.
138. Kagerbauer SM, Martin J, Schuster T, Blobner M, Kochs EF, Landgraf R (2013): Plasma oxytocin and vasopressin do not predict neuropeptide concentrations in human cerebrospinal fluid. *J Neuroendocrinol* 25:668–673.
139. Altemus M, Fong J, Yang R, Damast S, Luine V, Ferguson D (2004): Changes in cerebrospinal fluid neurochemistry during pregnancy. *Biol Psychiatry* 56:386–392.
140. Modi ME, Connor-Stroud F, Landgraf R, Young L, Parr L (2014): Aerosolized oxytocin increases cerebrospinal fluid oxytocin in rhesus macaques. *Psychoneuroendocrinology* 45:49–57.
141. Mens WB, Witter A, van Wimersma Greidanus TB (1983): Penetration of neurohypophyseal hormones from plasma into cerebrospinal fluid (CSF): Half-times of disappearance of these neuropeptides from CSF. *Brain Res* 262:143–149.
142. Macdonald KS (2012): Sex, receptors, and attachment: A review of individual factors influencing response to oxytocin. *Front Neurosci* 6:194.
143. Bakermans-Kranenburg MJ, van IJzendoorn MH (2014): A sociability gene? Meta-analysis of oxytocin receptor genotype effects in humans. *Psychiatr Genet* 24:45–51.
144. Bartz JA, Zaki J, Bolger N, Ochsner KN (2011): Social effects of oxytocin in humans: Context and person matter. *Trends Cogn Sci* 15:301–309.
145. Guastella AJ, Hickie IB, McGuinness MM, Otis M, Woods EA, Disinger HM, et al. (2013): Recommendations for the standardisation of oxytocin nasal administration and guidelines for its reporting in human research. *Psychoneuroendocrinology* 38:612–625.
146. Baroncini M, Jissendi P, Balland E, Besson P, Pruvost JP, Francke JP, et al. (2012): MRI atlas of the human hypothalamus. *NeuroImage* 59: 168–180.
147. Mai J, Paxinos G, Voss T (2007): *Atlas of the Human Brain*, 3rd ed. London: Academic Press.